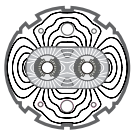

LHC Project Note 391

2006-11-10

Maciej.Chorowski@cern.ch

Radiation Tolerance Tests of Ultrasonic Oxygen Deficiency Sensors

K. Brodziński*, M. Chorowski*, W. Gizicki*, A. Jedrusyna*, W. Ostropolski*, G.Riddone

CERN, AT-ACR

*Wrocław University of Technology, Poland

Keywords: ODH, ultrasonic detector, irradiation test

Abstract

The Large Hadron Collider (LHC), presently under construction at CERN, will contain about 96 tons of high-density helium (liquid and supercritical), mostly located in the underground components of the LHC machine. To detect a dangerous decrease of oxygen concentration in the atmosphere caused by a potential release of helium, the Oxygen Deficiency Hazard Detection system will be applied for the LHC operation in the tunnel and other selected areas. The oxygen concentration is derived on the assumption that the gas added to the air is helium alone. A novel concept of oxygen deficiency detection system, built at the Wroclaw University of Technology (WUT) in Poland, allows verifying the oxygen concentration in the air by means of sound velocity measurements. The paper describes the design and functionality of two prototypes of ultrasonic ODH detection system tested by the WUT. In order to qualify the systems to be used in the LHC tunnel, the stability of ultrasonic transducers and electronics has been checked under radiation in an environment similar to that predicted for the LHC. At the beginning both systems have been tested in TCC2 test radiation zone at CERN. The complementary test, was performed in Institute of Atomic Energy (IEA) in Poland.

1. INTRODUCTION

The Large Hadron Collider (LHC), presently under construction at CERN, will contain about 96 tons of high-density helium (liquid and supercritical), mostly located in the underground components of the LHC machine.
The cryogenic system of the LHC machine is characterized by specific design features, which make it inherently safe. Nevertheless, as it was specified in the Preliminary Risk Analysis [1], some of potential LHC cryogenic system failures followed by helium discharge to the tunnel and potential decrease of the oxygen concentration below the safety level of 18 % in underground tunnel and caverns cannot be excluded. As a result of the previous studies the recommendations for oxygen deficiency monitoring system have been formulated. The system will comprise about 200 ODH detectors installed along the LHC machine. Standard, commercially available ODH detectors usually operate on the galvanic cell principle and they measure directly the oxygen concentration.

The novel concept of oxygen deficiency detection base on sound velocity measurement [2]. The oxygen concentration is derived on the assumption that the gas added to the air is helium alone. The sound velocity a in a perfect gas mixture is given by equation (1).

$$a = \sqrt{\kappa R T} = \sqrt{\left(\frac{1}{\sum \frac{z_i}{\kappa_i - 1}} + 1 \right) \cdot \frac{\bar{R} T}{\sum z_i M_i}} \tag{1}$$

Where: κ - adiabate exponent, T – temperature, R - gas constant of the mixture, $\bar{R}$ universal gas constant and z_i and M_i molar concentration and molar weight of the i-th component respectively.
The dependence of sound velocity versus helium concentration in the helium-air mixture (full line), calculated from equation (1) at 300 K is presented in figure 1. A dotted line shows a sound velocity in the air (the reference line). As presented in figure 1, the sound velocity for helium-air mixture depends strongly on the mixture composition and it is about three times higher for pure helium than for the air.

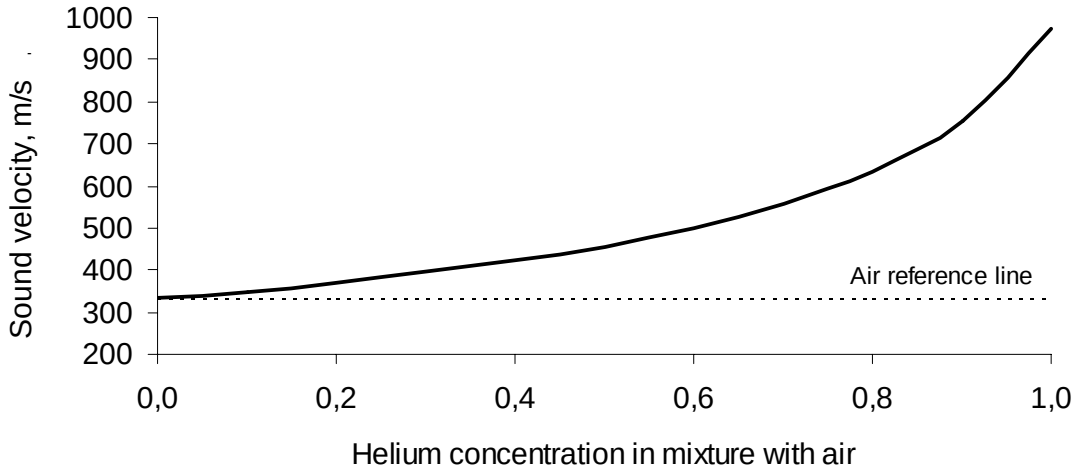

Fig. 1. Sound velocity as a function of helium concentration in the air

Three prototypes of ultrasonic sound velocity measurements system were designed and built at the Wroclaw University of Technology. The systems are predicted for detection of helium in the air with quantity sufficient to cause the Oxygen Deficiency Hazard.

2. AIM OF THE TEST

The aim of the test was to verify a long-term stability of ultrasonic transducers and electronics in radiation environment.
The first part of the test was carried out at CERN TCC2 irradiation facility in radiation environment similar to that predicted for the LHC.
The second, complementary part, was carried out at the Institute of Atomic Energy (IEA), in Otwock-Swierk near Warsaw in Poland.

3. TCC2 IRRADIATION FACILITY

The TCC2 radiation test zone is situated in the primary Target Hall in the north area of the SPS complex at CERN. In the target hall, protons at 400 GeV are dumped on targets to generate secondary particles for the fixed target experiments situated further down the stream. The radiation produced is typical of a proton accelerator. It includes mainly gammas, neutrons (both low- and high energy) and some high-energy particles.
A radiation environment in this facility is very similar to that predicted for the arcs of the LHC. It is the same for particle fluences above E_{cut} = 1 MeV. In case of particle fluences with E_{cut} < 1 MeV, the TCC2 test area has a higher neutron dose ratio than the LHC radiation environment. In this case SEU problems experienced under TCC2 testing would be greater than at the LHC.
TCC2 irradiation facility will provide good radiation environment for testing electronics, which could by used in the LHC [3].

4. TEST SET UP

Three ultrasonic measurement systems have been designed and constructed at the Wroclaw University of Technology. Two of them (unit #1 and unit #2) are working at 108.5 kHz frequency and the third one (unit #3) at 40 kHz frequency.
The design of unit #1 and unit #2 were the same, but the tests of the devices were performed in a different way. The unit #1 was operated in a passive mode, i.e. it was triggered once a week for several minutes. The unit #2 was tested in an active mode. It worked in a continuous way and the results were stored every 15 minutes.
The construction of unit #3 differed from units #1 and #2 and it was operated in a passive mode, similarly to device #1.

4.1. Technical description of the ultrasonic system working at 108.5 kHz (unit #1 and unit #2)

A test set-up is shown schematically in figure 2.

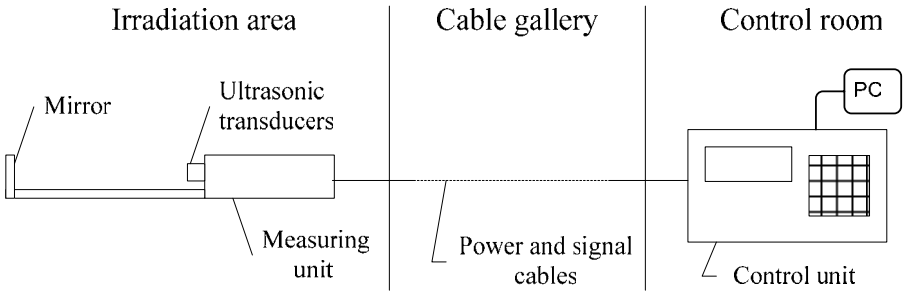

Fig. 2. Test set-up working at 108.5 kHz schematic view

The system consist of three parts:

– the sound-velocity measuring unit, placed directly in irradiation area, in the target hall of the SPS accelerator (in the vicinity of PMITC09 dosimeter).

– a bunch of supply and signal cables, located in a shaft joining the accelerator tunnel with the surface SPS facilities.
– the control unit connected to the PC, placed in the SPS control room; the unit has triggered the measurements, performed the readout of the results and transmitted the data to the PC.

The sound velocity measuring unit, placed in the irradiation zone, comprises two piezoelectric ultrasonic transducers (a transmitter and a receiver) working at 108.5 kHz resonance frequency, electronics and Ni160 thermocouple. The electronics system is shielded with 12 layers of one-millimeter sheet of lead, of a total thickness of 12 mm. The whole device is closed in the aluminium housing. The elements located outside the shield are only the thermocouple sensor and the transducer ceramic endings. A mirror placed on an extension arm of 80 mm length reflects signals emitted by the transmitter to the receiver - see figure 3 and figure 4.

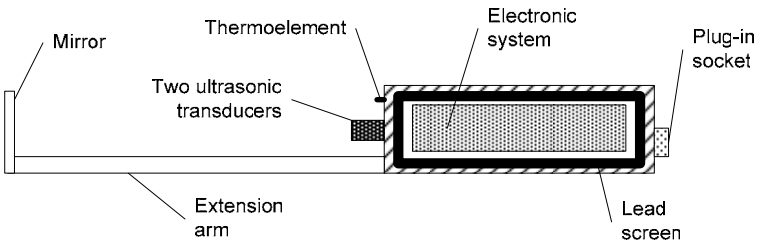

Fig. 3. Sound-velocity measuring unit working at 108.5 kHz resonance frequency

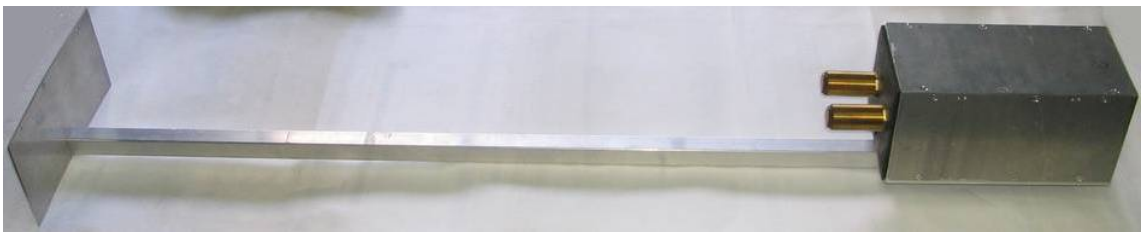

Fig. 4. General view of the sound-velocity measuring unit working at 108.5 kHz resonance frequency, placed in the TCC2 irradiation zone

After triggering the measurements by the control unit located in the SPS control room, the electronic system has to emit an ultrasonic burst and receive a signal reflected from the mirror. The received and processed signal is sent back to the control unit to evaluate the time of the wave propagation along a known distance. Additionally the unit is measuring the air temperature in the ultrasonic wave propagation area.
The electronic system of the emitter consists of a quartz stabilized frequency oscillator, a modulo-16 counter, a logical gate and a power amplifier. The receiver path consists of a selective amplifier, an amplitude detector and a 2-threshold comparator.
The communication between the measuring unit and the control unit is enabled by RS 485 port, guaranteeing resistance to electromagnetic interferences. Figure 5 shows a block diagram of the electronic system of the measuring unit.

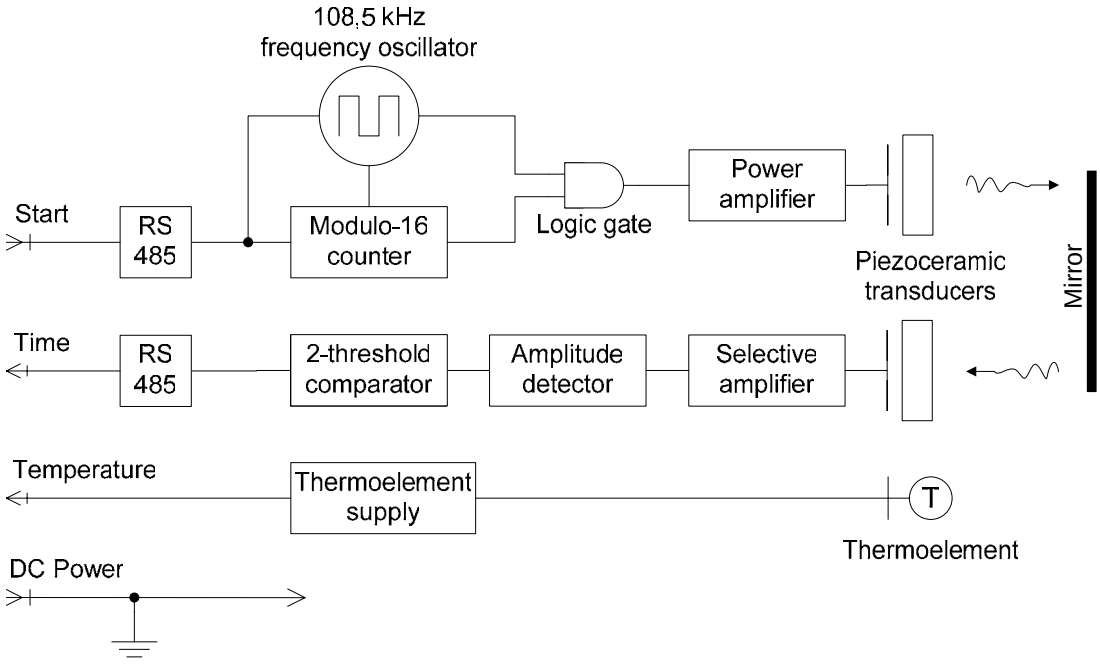

Fig. 5. Block diagram of the electronic system of the sound-velocity measuring unit placed in the TCC2 irradiation zone

The control unit, placed in the BA80 control room is shown in figure 6. The unit was connected with a PC, imposing the frequency of the measurements and storing the results.

Fig. 6. The control unit placed in the BA80 control room

The electronic system of the control unit is made of a SIEMENS SAB 80537 microprocessor, E-PROM memory chip, LCD, a keyboard, communication ports to measuring unit (RS 485) and to the computer (RS 232) and a power supply. A block diagram of the control unit is shown in figure 7.

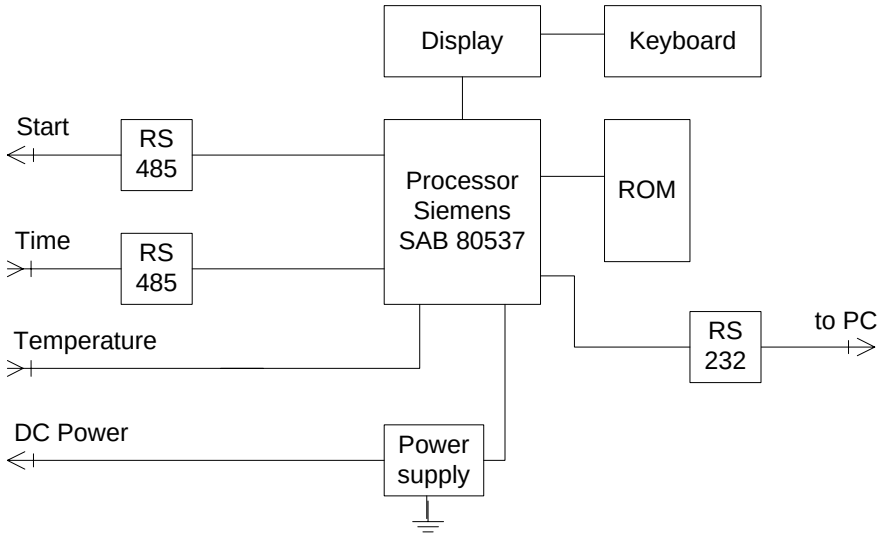

Fig. 7. Block diagram of the electronic system of the control unit placed in the BA80 control room

There is appropriate software installed (E-PROM) in order to start measurements in a specific time period and to preliminary data handling. After beginning the measurement, the microprocessor is sending START signal to the measuring unit placed in the accelerator tunnel. In the measuring unit a quartz stabilized frequency oscillator together with a modulo-16 counter are generating wave pocket consisting of 16 rectangular pulses with 108.5 kHz frequency. Every impulse, which has a period of $9.2 \cdot 10^{-6}$ s (9.2 μs), has peak-to-peak amplitude of 300 V without a constant component. The amplitude is symmetrical to eliminate constant initial stress of the transmitter crystal. The wave pocket is then amplified and led to the piezoelectric transducer, where an ultrasonic wave is generated. The peak power is 40 W, with impedance of the transmitter crystal 300 Ω (for the resonance frequency 108.5 kHz).
The ultrasonic wave, after reflecting in the mirror, is reaching the receiving transducer, in which it is changed again to an electric signal. This signal is then amplified in selective amplifier with mid-band frequency 108.5 kHz and a bandwidth 2 kHz (for -3 dB loss on the endings of the range). The amplification factor is about 100 dB (about 100 000 $^{V}/_{V}$).
The received signal is going then to the amplitude detector and then to 2-threshold comparator, which is reading out two points on an accretion curve of the signal amplitude. Both comparator output signals are then sent back to the microprocessor in the control unit.
The whole operation of starting the measurement and reading out answers is repeated 100 times and then the microprocessor, using algorithm written in E-PROM chip, is computing average response times from all measurements and on the basis of them is approximating the precise time of flight of the ultrasonic wave between the transducers.
Time of propagation measured in that way is dependent both on the air composition and the temperature. To eliminate the temperature effect, a Ni160 thermocouple is installed. The measured propagation time is normalized to a base temperature T_0 = 289 K (16 °C) conditions according to the formula:

$$t_0 = t\sqrt{\frac{T}{T_0}} \tag{2}$$

t_o - time of propagation in base temperature, s;
t - real, measured time of propagation, s;
T - measured temperature, K;
T_o - base temperature, K.

The measured parameters – real time of propagation and temperature are presented on LCD display and sent to the PC data acquisition system.

4.2. Technical description of the ultrasonic system working at 40 kHz (unit #3)

The measuring system consists of the metal chassis with ultrasonic transducers and two electronic modules: No.1 located in TCC2 irradiation zone and No.2 located in the BA80 control room. The communication between modules is commenced over RS-485 interface using standard twisted pair of wires (120 Ohm impedance, 2 pairs). Another pair of wires is used for supplying the power (+12V DC) from Module No. 2 to No. 1. The maximum distance between modules cannot exceed 1500 m.

A scheme of the ultrasonic measurement system (unit #3) is shown in figure 8.

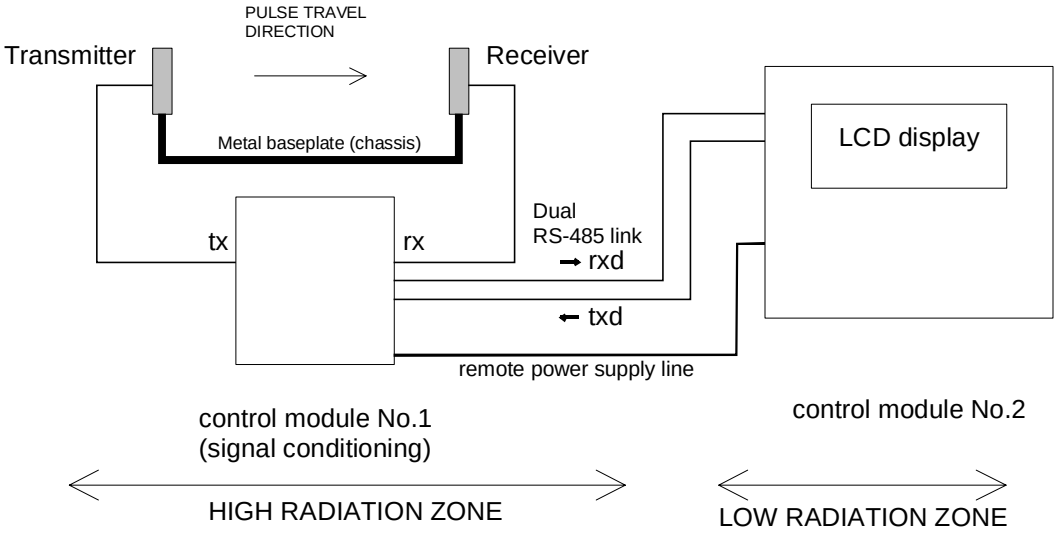

Fig. 8. Test set-up working at 40 kHz schematic view (unit #3)

The system #3 uses cheap 40 kHz transducers for generation and detection of the ultrasonic signal. The transducers are mounted on the metal frame (chassis) in the fixed distance of 0.62 m. An average time of flight (TOF) when measured in the air is about 2 microseconds.
The module No.1 includes the control interface and the analogue signal conditioning circuits (60 dB amplifiers with high-pass filter and amplitude demodulator).
Module No. 2 includes the power supplies for both modules, a microcontroller module and the LCD display for TOF and sound velocity visualization. The Atmel AVR 90S8515 microcontroller was used for generation of 40 kHz pulses and TOF measurement with its internal timers. The internal structure of the module No. 1 is shown in Fig. 9.

Module No. 2 includes the microcontroller circuit for data acquisition and visualization. That module generates 40 kHz bursts and sends them to module No. 1 (txd signal). The LCD display shows both TOF and the sound velocity. The internal structure of the module No. 2 is shown in Fig. 10.

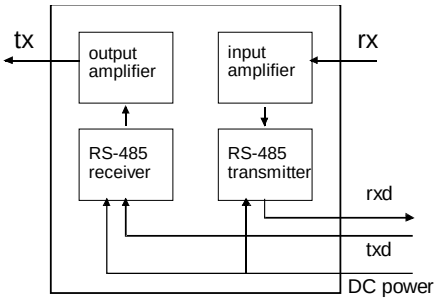

Fig. 9. The block diagram of the module No. 1 (unit #3)

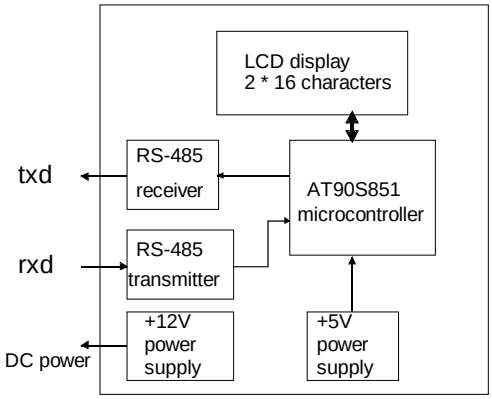

Fig. 10. The block diagram of the module No. 2 (unit #3)

The signal sent from module No. 2 (txd) is amplified and send to ultrasonic transmitter (tx signal). The received rx signal from the receiver is amplified and demodulated, then sent back to the module No. 2 (rxd signal). The present version of circuit included no temperature sensor. Fig. 11 shows the waveforms tx, rx, rxd and txd respectively.

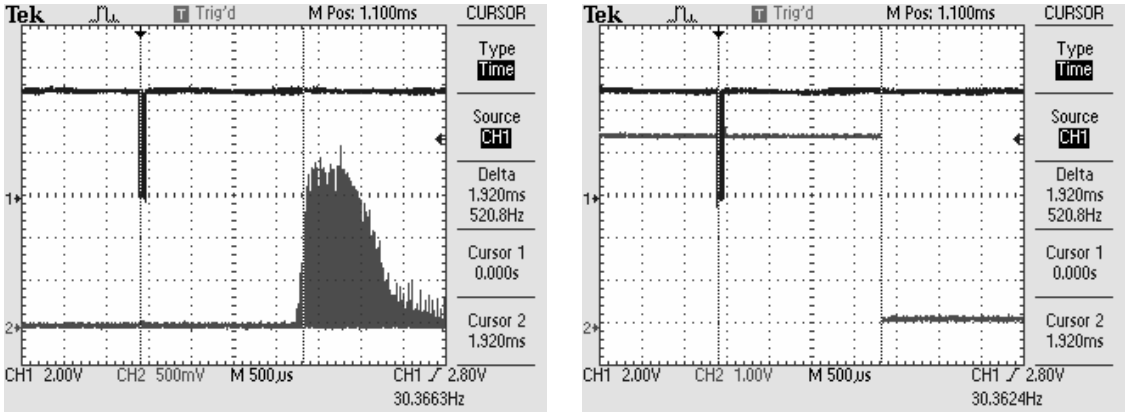

i) ii)

Fig. 11. The waveforms in the module No. 1 (unit #3):
i) tx (top) and demodulated rx (bottom) ii) tx (top) and rxd (bottom).

Basic specification of the system:

Dimensions:

Chassis with transducers - 700x100x100 mm
Electronic module No. 1 - 150x150x100 mm
Electronic module No. 2 - 200x200x150 mm
Power supply (module No. 2 only) – 230 V, 5W

Total weight (chassis + modules No. 1,2) - 3 kg

The complete unit #3 is presented in fig. 12.

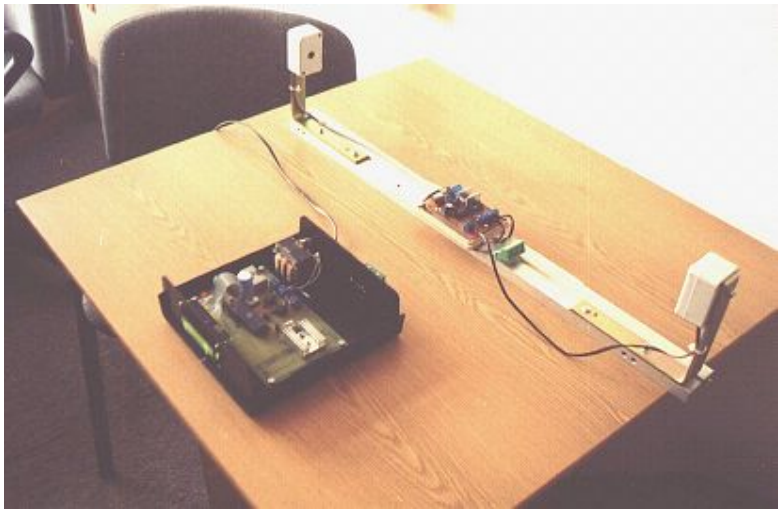

Fig. 12. The complete unit #3 (top case removed).
Module No. 2 on the left, Module No. 1 fitted onto metal chassis on the right.
Ultrasonic transducers visible on the end of chassis.

5. RESULTS

The measurements took place between May and November 2003. As described previously the Unit #2 was working in an active mode, it means that it was automatically and continuously triggering the measurements. The results were stored every 15 minutes. Unit #1 and unit #3 were working in a passive mode. They were switched on manually and the measurements took place once a week, according to the accelerator weekly breaks in the operation. The passive systems were switched on and off in the absence of the beam when the access to the tunnel was allowed. From a human safety point of view, the monitoring of ODH is not a must when the accelerator is active and the personnel are not allowed to be present in the tunnel. Such operation mode may be recommended for the LHC.

Unit #1, passive mode of operation.
The system was triggered weekly for one hour and the results are shown in table 1 (Appendix A) and figure 13.

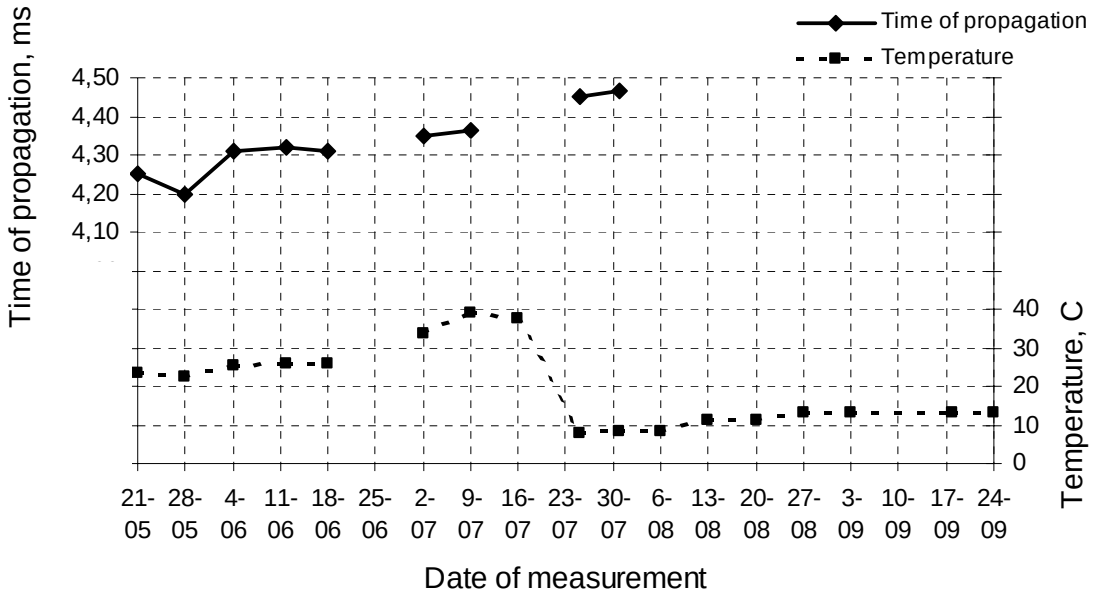

Fig. 13. Results from the passive mode system working at 108.5 kHz frequency (unit #1)

Unit #2, active mode of operation.

The results registered for unit #2 operated in an continuous active mode are given in table 2 (Appendix A). The data were stored every 15 minutes and then the average value for each day was calculated. The columns are described in the same way like for table 1.
Similarly as in the previous case (passive mode), a chart of values of time of propagation and readout temperature as a function of time of active mode system work is shown in figure 14.

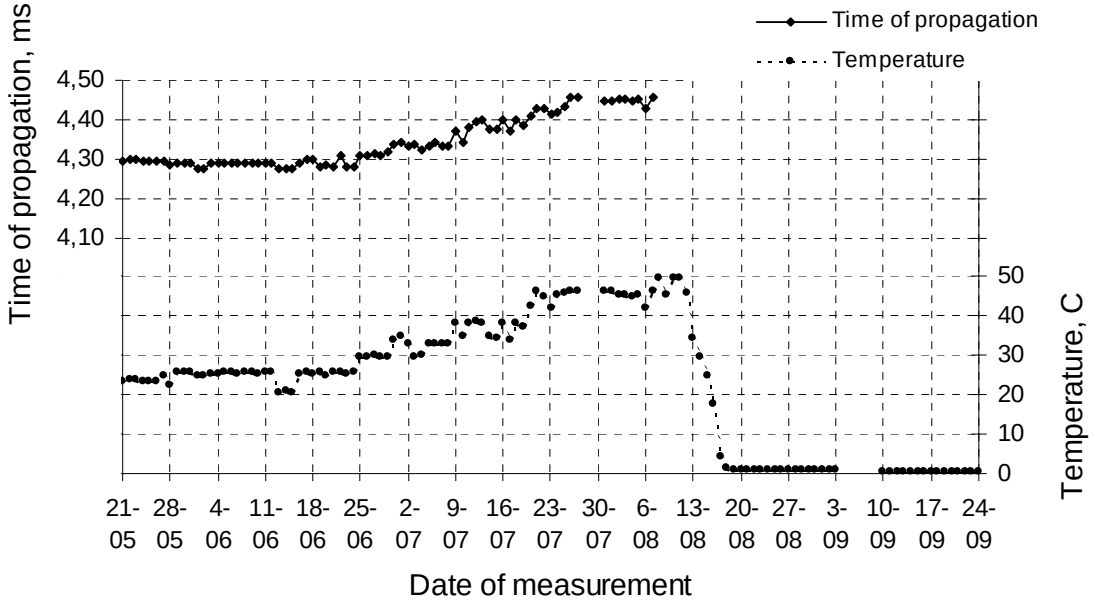

Fig. 14. Results from the active mode system (unit #2)

The comparison of the results registered for both systems is given in figure 15. The measured sound velocities are converted to the base temperature T = 16 °C. The obtained results are very close to each other and both systems gave good values. The two systems operated reliably for a very similar time before they failed.

It can be concluded that continuous triggering of the active system did not cause additional danger of the electronics degradation due to the ionizing radiation.

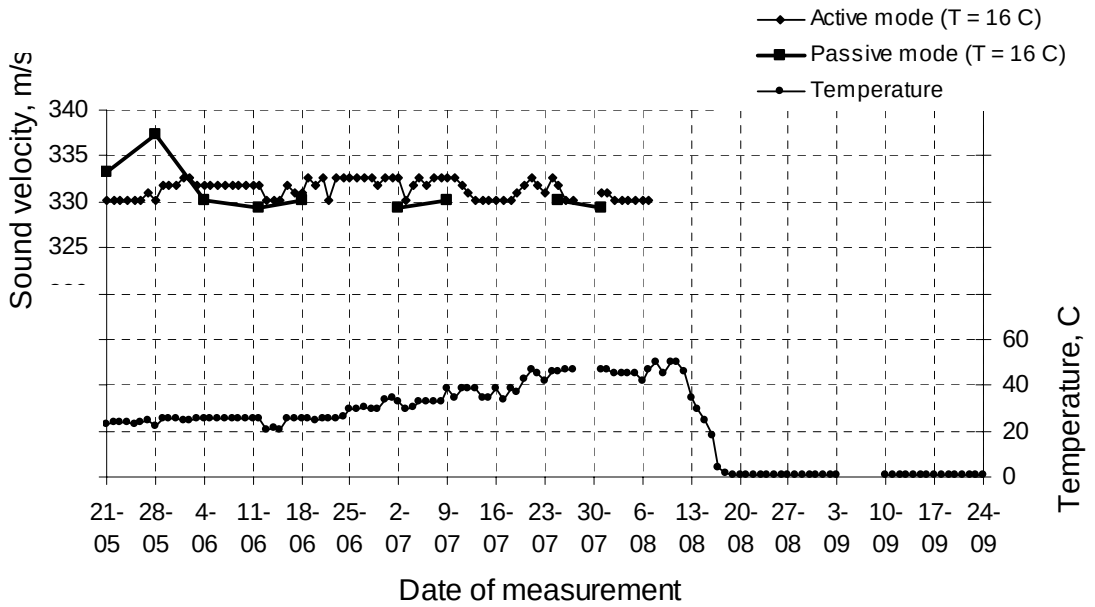

Fig. 15. Comparison between passive and active mode systems (units #1 & #2), velocity of sound converted to the base temperature T = 16 °C

Unit #3, passive mode of operation.

The results from the unit #3 are shown in table 3 (Appendix A). The results were registered weekly. The unit #3 was not equipped with a temperature measurement and compensation function. The only measured value was the propagation time between the two transducers. The sound velocity was calculated.
Values of the sound velocity as a function of time of the measurement system work is shown in the chart in figure 16.

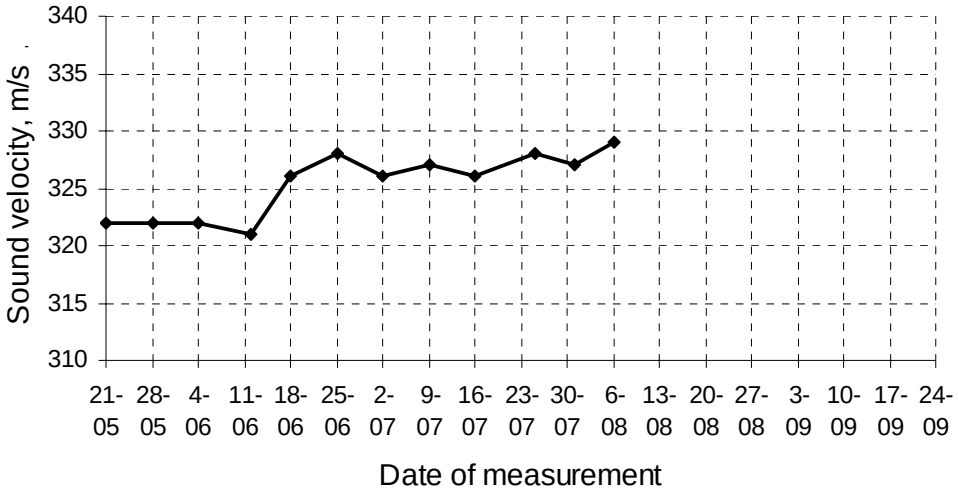

Fig. 16. Results from the passive mode system (unit #3)

6. STABILITY OF THE READOUTS

Unit # 1 (passive mode)
The largest measured deviation in the average values of the measured propagation time was 0.08 ms.
This difference corresponds with helium concentration of about 4 % in the air and the corresponding oxygen concentration of 20.16 % (drop by 0.84 %)

Unit # 2 (active mode)
In case of unit #2, the stability study (assessment) was made on the basis of statistical analysis, because of the big number of autonomous (independent) measurements (Appendix A, tab.2).
The average time of propagation $\bar{t}$ for *n* measurements

$$\bar{t} = \frac{1}{n}\sum_{i=1}^{n} t_i = 4.224 \text{ ms} \tag{3}$$

The mean square error was calculated as the standard deviation

$$u_A = \sqrt{\frac{1}{n-1}\sum_{i=1}^{n}\left(t_i - \bar{t}\right)^2} = 0.012 \text{ ms} \tag{4}$$

The measuring error for the confidence interval of 95 % was calculated with the coefficient $k = 2$

$$U = k \cdot u_A = 0.024 \text{ ms} \tag{5}$$

In fact, the largest measure deviation in the average value of the measured time of propagation was inside the measuring error range and was 0.02 ms.
That difference corresponds with helium concentration of about 1 % in the air and the corresponding oxygen concentration of 20.79 % (drop by 0.21 %)
The variations in the measured propagation times correspond with the variations in oxygen concentration in the air below 0.5 % - compare figures17 and 18. There is no danger to trigger false alarms of ODH.

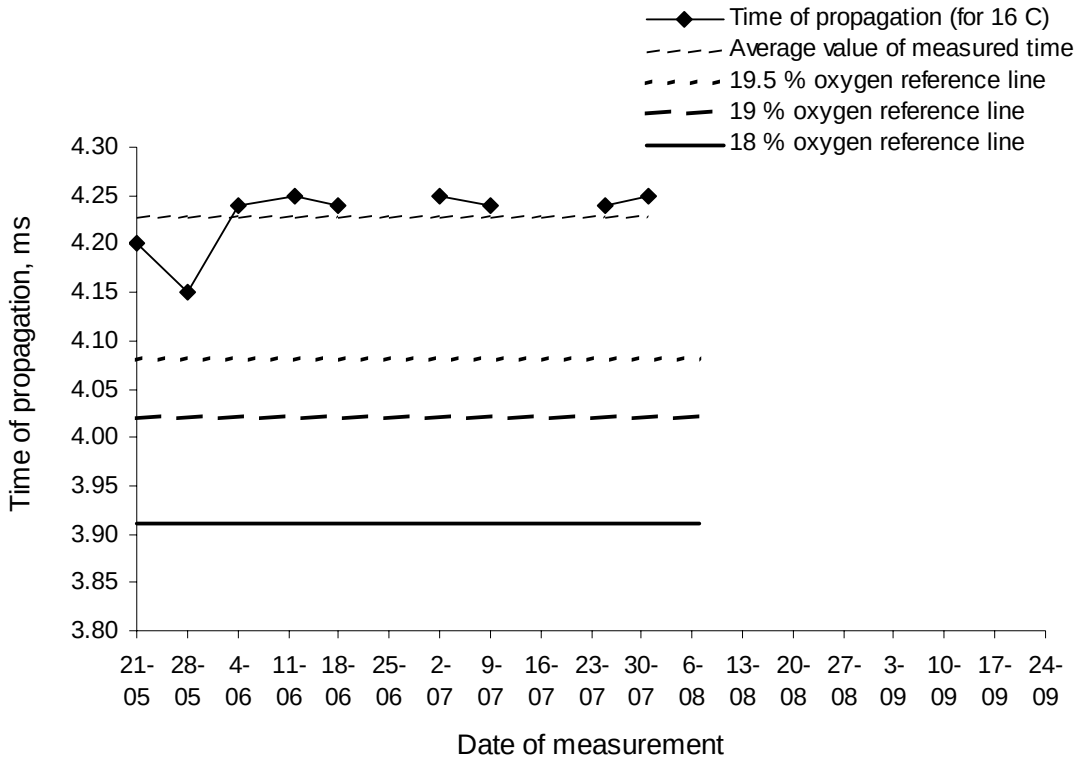

Fig. 17. Comparison between average values of propagation time measured by unit #1 (passive system) and 18, 19, 19.5 % oxygen concentration thresholds.

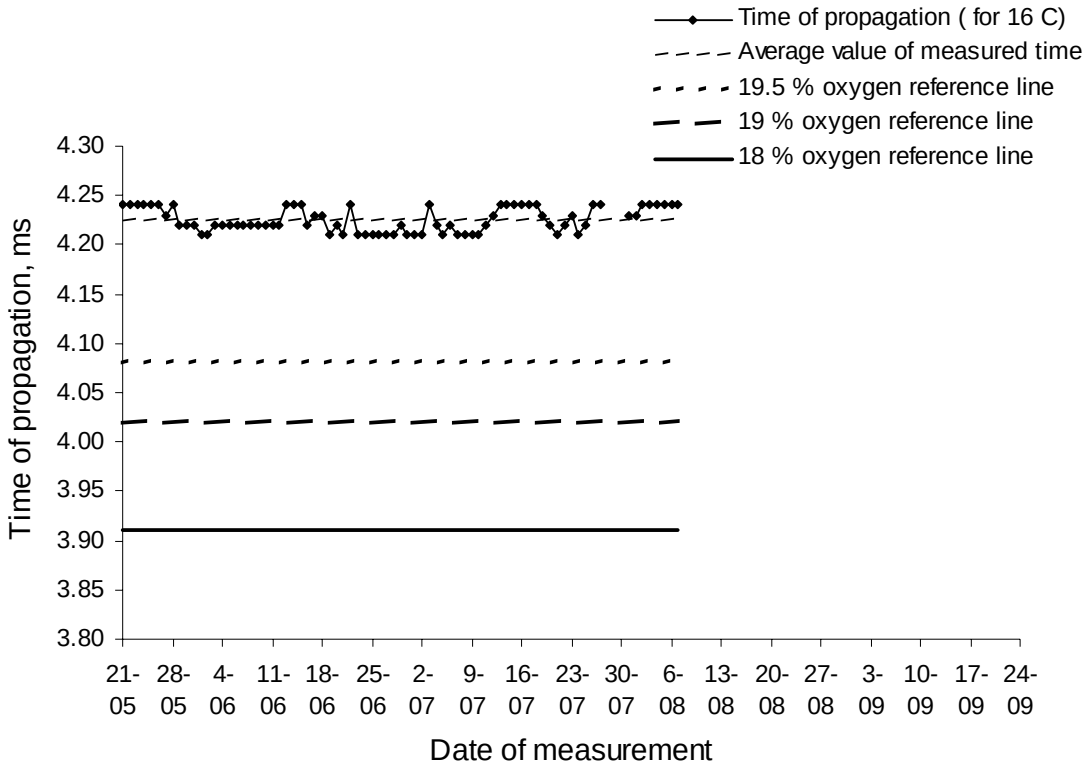

Fig. 18. Comparison between average values of propagation time measured by unit #2 (active system) and 18, 19, 19.5 % oxygen concentration thresholds.

Unit # 3 (passive mode)
In this case, there was no temperature compensation and the analysis of the readouts stability was not performed.

7. ACCUMULATIVE DOSE ABSORBED

The accumulative dose absorbed in Sv measured by PMITC09 dosimeter is shown in figure 19. The dose is slightly lower than the one measured in year 2002. The corresponding accumulative doses in Gy measured in 2002 and estimated for 2003 are in a very big discrepancy – see figure 20. The very low value estimated as a 2003 Gy dose cannot be trusted. To estimate accumulative dose absorbed by the acoustic sensors during their operation in the TCC2 radiation test zone we propose to treat the measured value in Sv as equal to the dose absorbed in Gy. The results of the cumulative radiation dose estimation are given in table 4 and figure 21.

Tab. 4. Cumulative absorbed doses until failure for each measurement system

Measurement system	Absorbed doses in TCC2 test area in 2003, close to PMITC09	
	measured in 2003 Sv	estimate for 2003 Gy
Unit #1 (passive mode)	66	66
Unit #2 (active mode)	70	70
Unit #3 (passive mode)	68	68

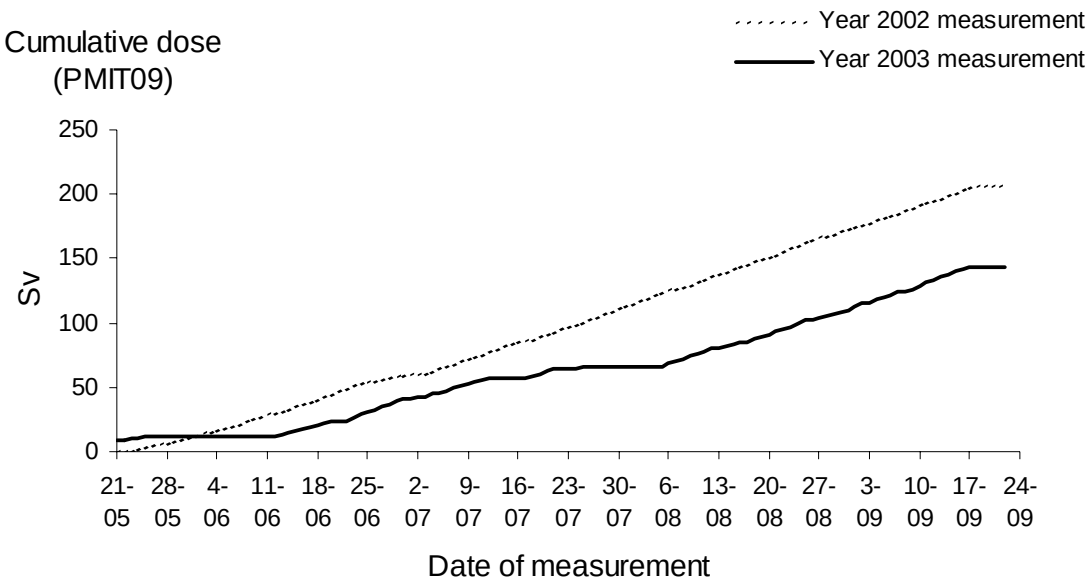

Fig. 19. Comparison between measured cumulative doses in sieverts measured in years 2002 and 2003

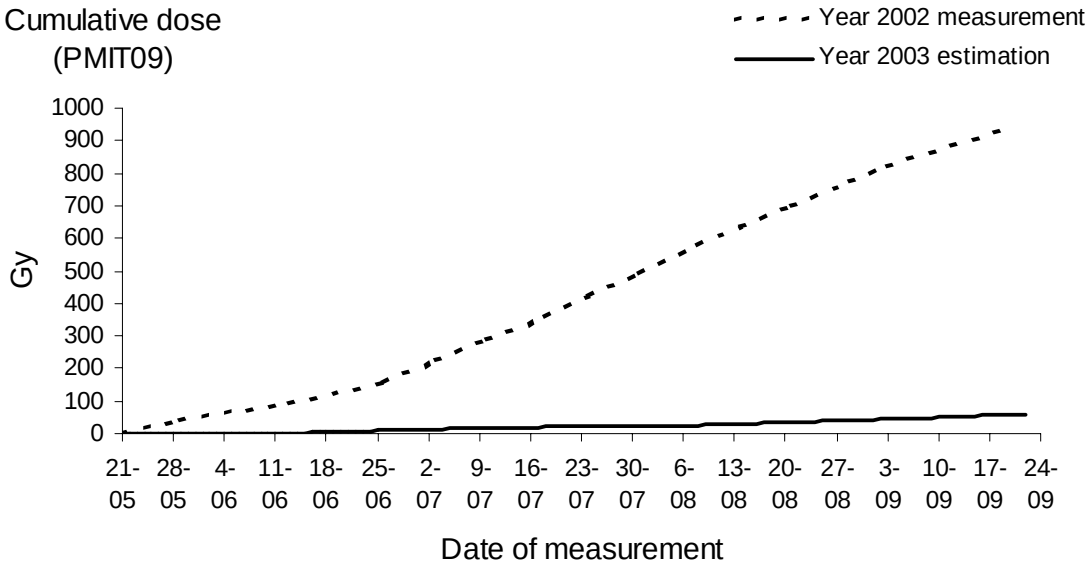

Fig. 20. Comparison between cumulative doses in grays measured in year 2002 and estimated in year 2003

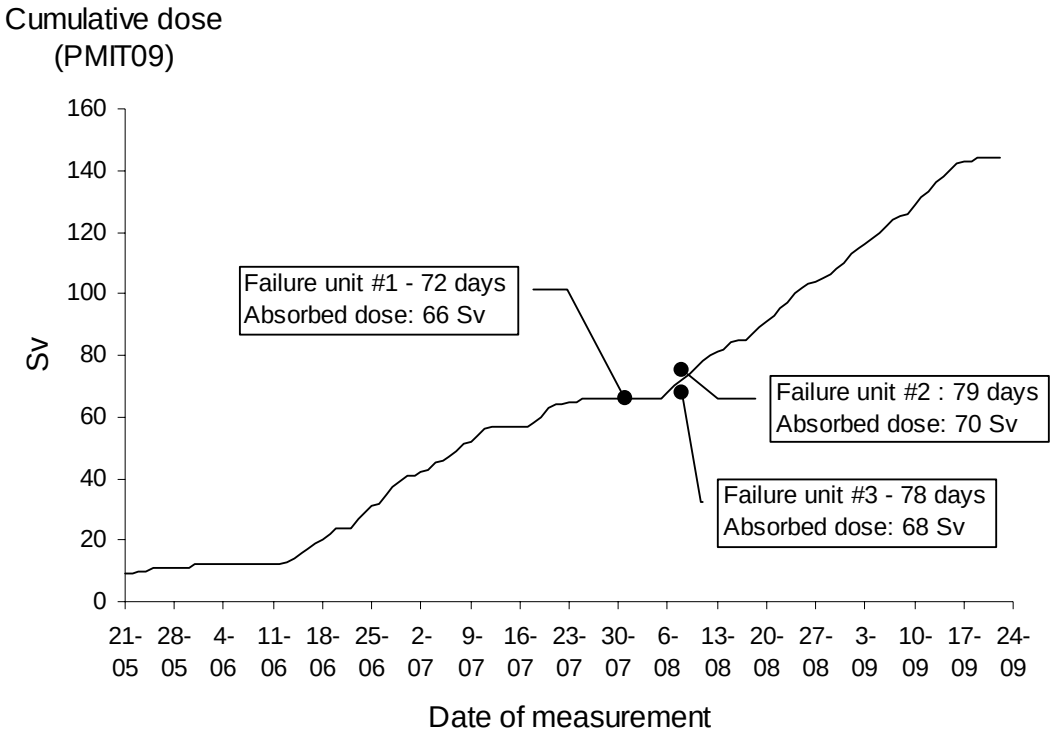

Fig. 21. Graphic display of the results

8. RELIABILITY ANALYSIS

After the end of the investigation all three ultrasonic measurement systems have been shipped back to Poland. After the failure analysis made at the Wroclaw University of Technology it was concluded that:
All systems which were located in BA-80 control room remained in working order and kept full functionality. However, the sound-velocity measuring units, which were placed directly in the irradiation area, were damaged.
As a result of damage research it was stated that:

Unit #1 & #2 (with lead shielding)

i) Piezoceramic ultrasonic transducers stayed operative in both units

ii) The receiver path consisted of selective amplifier, amplitude detector and 2-threshold comparator stayed operative in both units

iii) The power amplifier of the transmitter stayed operative in both units

iv) The modulo-16 counter in both units failed
Symptoms: out of order, total damage
Possible cause: thermal damage

v) The input amplifier in the thermoelement supply in both units failed. First loss of stability for few days, then failure
Symptoms: out of order, total damage
Possible cause: thermal damage

The most probable reason for all chips' damage was the over standard increase in the temperature, which gained 50 ºC at the moment of the breakdown. Radiation impact is appearing to be insignificant, however it was possible that it had an assisting importance.

The following facts support it:
- all the chips broke down during the highest temperature,
- broken electronic elements were standard class - not resistant to work in raised temperature,
- the failure of the counter caused the continuous transmission of the ultrasonic wave. It caused increased heat release from the power transistors inside the housing and gave a bigger rise of temperature. As it is shown in tab. 2 (Appendix A) from the moment of counter-failure (07.08.2003) the work of the thermoelement supply was first unstable and then failed,
- the rest of electronic components remained functional without any deteriorations typical for the radiation damage; in particular the non-shielded piezoceramic ultrasonic transducers with zirconium admixture, which is radiation-sensitive, stayed operative.

Unit #3 (without lead shielding)

i) CMOS operation amplifier TLC272 failed.
Symptoms: very low gain and increased noise level.
Possible cause: destruction of the gate oxide layer in the CMOS transistors.

ii) Two SN75176 RS-485 transceivers failed.
Symptoms: RS-485 transmitters in both chips failed. The amplitude of the transmitted RS-485 was reduced by about 50% and additional non-symmetrical DC component appeared. Moreover, parasitic oscillations in the transmitted RS-485 signal appeared. Both RS-485 receivers remained functional.
Possible cause: damage of SN75176 output stage including transistors and Schottky diodes.

iii) Other elements in the unit remained functional.

In this case failure of the unit was caused by partial degeneration of dice, what is typical for irradiation. That unit was free from leaded shield. The rise of temperature was the additional cause.

There was a considerable impact of radiation in each testing unit, but it was the direct reason of failure only in non-shielded unit #3. In lead-shielded units #1 & #2 the main reason was the temperature rise.

Indications in order to increase reliability of the measuring units

In order to increase reliability of applied measuring instruments it is necessary to:

- apply electronic elements coming from known and checked manufacturers, with raised climatic class,
- the current type of modulo-16 counter can be replaced with serial carry counter,
- keep the lead shielding and additionally screen the piezoceramic transducers,
- apply a solution of the housing, facilitating exchange of warmth between the electronic setup and the environment.

9. ADDITIONAL TEST AT NUCLEAR REACTOR

Because of the uncertainty in estimated values of accumulative absorbed doses in Gy, an additional irradiation test was advisable. There was no possibility to repeat the tests at TCC2 facility due to technical reasons.
The experiment was carried out at the Institute of Atomic Energy (IEA), Otwock-Swierk near Warsaw, Poland.
The position of measuring units was placed near the atomic core from the testing reactor.

The nominal parameters of the beam of radiation are:
- Kerma rate from gamma rays: ca. 0.3 Gy/h,
- Kerma rate from neutrons (mainly fast neutrons): ca. 0.04 Gy/h,
- Thermal neutron fluence rate: 3.5E+7 $cm^{-2}s^{-1}$,
- Epithermal neutron fluence rate: 5.0E+5 $cm^{-2}s^{-1}$.

Only the ultrasonic system working at 108.5 kHz (unit #1 and unit #2) was used for the test - without any modifications, only after repair. Both units worked in active mode (continuous measurement) and were placed (one after another) in the mouth of a horizontal irradiation channel. Each unit had two radiation detectors located at the front and at the back of its housing. The test was performed from 16.07.2005 to 22.09.2005 (with a technical break from 30.07.2005 to 7.08.2005). Absorbed doses after the test are given below and in the table 5.

Unit #1 - front detector
D_gamma = 95 Gy, D_thermal_neutron = 13.2 Gy, D_fast_neutrons = 9 Gy
Unit #1 - rear detector
D_gamma = 56 Gy, D_thermal_neutron = 5.1 Gy, D_fast_neutrons = 3 Gy
Unit #2 - front detector
D_gamma = 66 Gy, D_thermal_neutron = 9.2 Gy, D_fast_neutrons = 6 Gy
Unit #2 - rear detector
D_gamma = 44 Gy, D_thermal_neutron = 4.3 Gy, D_fast_neutrons = 3 Gy

Tab. 5. Cumulative doses absorbed by the unit #1 & unit #2

	front detector Gy	rear detector Gy	average inside Gy
Unit #1	117.2	64.1	**91**
Unit #2	81.2	51.3	**66**

Both ultrasonic measurement systems remained operative and functional during the test and after the test was over. No deterioration of dice was found. The time of propagation, measured

during the entire test, corresponded with the expectations and was stable all the time. Values of time of propagation and readout temperature as a function of time of both systems' work is shown in figure 22.

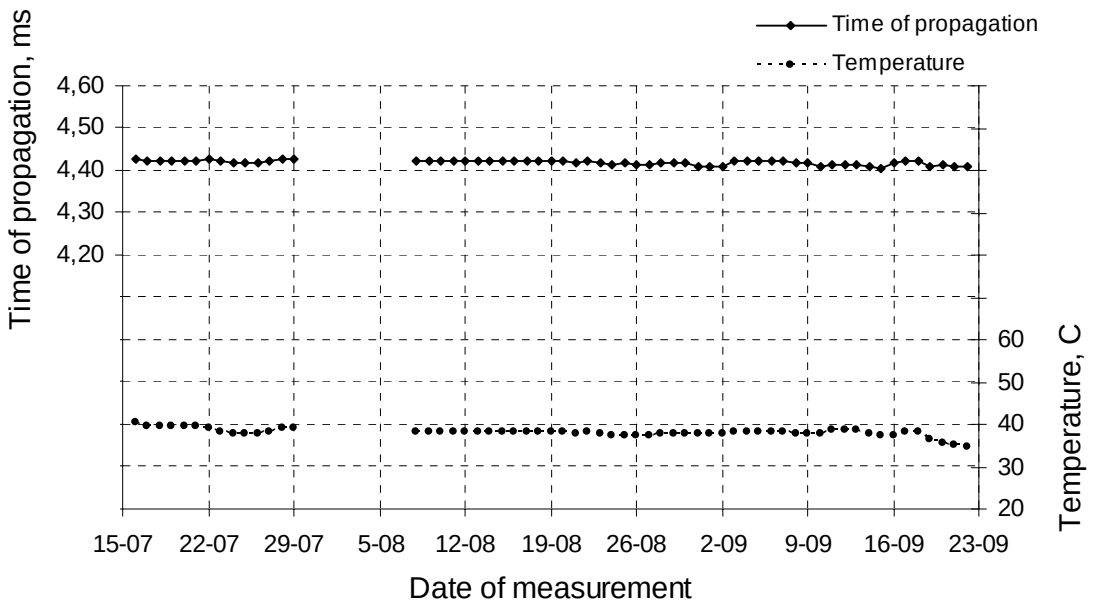

Fig. 22. Time of propagation and readout temperature from both of the systems (unit #1 % unit #2) tested at nuclear reactor

10. CONCLUSIONS

Prototype acoustic sensors to monitor helium presence in the air have been successfully designed, constructed and commissioned. The sensors work on the principle of sound wave propagation time measurement. They are composed of two ultrasonic transducers, electronics and data acquisition system.
The sensors have been tested in the TCC2 radiation test zone in an environment similar to that predicted for the arcs of the LHC. The accumulative dose absorbed was estimated, but at least 66 Gy what corresponds with above 10 years of the LHC operation. In case of unit #1 & #2 it is still possible to expect engaging bigger doses of radiation. In an additional test at the testing reactor both units (#1 & #2) received up to 91 Gy and still remained operative and functional.
The readouts were very stable and there is no danger to provoke false alarms of ODH.
The developed technology can be considered to be used in the installations, where the oxygen deficiency hazard may be a result of helium release into the air.

The radiation tolerance tests should be continued for two reasons:
- The accumulative absorbed dose in Grays was not measured, but only estimated on the basis of measured dose in sieverts and compared to previous year's results. The further test at nuclear reactor gave better result but a radiation environment in that facility was not very corresponding with that predicted for the arcs of the LHC.
- The failure of measuring units #1 & #2 in TCC2 irradiation zone was caused by the excessive temperature increase and the radiation effect is still unknown.

11. ACKNOWLEDGEMENTS

The authors wish to thank K. Pytel from the Institute of Atomic Energy (IEA), Otwock-Swierk, Poland, for help in the radiation measurements.

12. REFERENCES

[1] - Chorowski M., Lebrun Ph., Riddone G., *Preliminary Risk Analysis of the LHC Cryogenic System*, Advances in Cryogenic Engineering 45 B, pp. 1309-1316, Plenum, New York, USA, 2000

[2] - Chorowski M., Gizicki W., Wach J., *Application of acoustic tomography in helium-air mixture content monitoring*, Proceedings of the Nineteenth International Cryogenic Engineering Conference (ICEC 19), Grenoble, France, 2002, Narosa Publishing House, New Delhi, 2003

[3] - Fynbo C. A., Stevenson G. R., *Qualification of the radiation environment in the TCC2 experimental Test Area*, LHC Project Note 235, Geneva, 15 December 2000

Appendix A

Tab. 1. Results of the measurements using the passive system (unit #1)

Date	Time	Time of propagation	Temperature	Time of propagation (after temperature compensation)	Sound velocity (after temperature compensation)
	days	ms	C	ms	m/s
21-05	0	4.27	23.5	4.20	333
28-05	7	4.21	22.6	4.15	337
4-06	14	4.31	25.6	4.24	330
12-06	22	4.30	25.7	4.25	329
18-06	28	4.31	25.7	4.24	330
25-06	35	-	-	-	-
2-07	42	4.39	33.5	4.25	329
9-07	49	4.42	39.0	4.24	330
16-07	56	-	37.8	-	-
25-07	65	4.18	7.8	4.24	330
31-07	71	4.19	8.1	4.25	329
6-08	77	-	8.1	-	-
13-08	84	-	11.2	-	-
20-08	91	-	11.2	-	-
27-08	98	-	13.4	-	-
3-09	105	-	13.4	-	-
18-09	120	-	13.4	-	-
24-09	126	-	13.4	-	-

Date	stands for	Date of the measurement, day and month of 2003 year;
Time	stands for	Time from the beginning of installation the system and begin of research to the moment of measurement, given in days;
Time of propagation	stands for	Time of ultrasonic wave propagation between the sending and the receiving transducer, given in milliseconds;
Temperature	stands for	Temperature of the air in the ultrasonic wave propagation area measured by a thermoelement, given in °C;
Time of propagation (after temperature compensation)	stands for	Time of ultrasonic wave propagation between sending and receiving transducer, after converting to the base temperature $T = 289$ K (16 °C), given in milliseconds;
Sound velocity (after temperature compensation)	stands for	Velocity of the ultrasonic wave propagation, after converting to the base temperature $T = 289$ K (16 °C), shown in meters per second;

Tab. 2. Results of the measurements using the active system (unit #2)

Date	Time	Time of propagation	Temperature	Time of propagation (after temperature compensation)	Sound velocity (after temperature compensation)
	days	ms	C	ms	m/s
21-05	0	4.29	23.3	4.24	330
22-05	1	4.30	23.9	4.24	330
23-05	2	4.30	24.0	4.24	330
24-05	3	4.29	23.5	4.24	330
25-05	4	4.29	23.3	4.24	330
26-05	5	4.29	23.5	4.24	330
27-05	6	4.29	24.9	4.23	331
28-05	7	4.29	22.4	4.24	330
29-05	8	4.29	25.6	4.22	332
30-05	9	4.29	25.6	4.22	332
31-05	10	4.29	25.6	4.22	332
01-06	11	4.27	24.9	4.21	333
02-06	12	4.27	24.9	4.21	333
03-06	13	4.29	25.5	4.22	332
04-06	14	4.29	25.5	4.22	332
05-06	15	4.29	25.6	4.22	332
06-06	16	4.29	25.6	4.22	332
07-06	17	4.29	25.5	4.22	332
08-06	18	4.29	25.6	4.22	332
09-06	19	4.29	25.6	4.22	332
10-06	20	4.29	25.5	4.22	332
11-06	21	4.29	25.6	4.22	332
12-06	22	4.29	25.6	4.22	332
13-06	23	4.28	20.8	4.24	330
14-06	24	4.28	21.1	4.24	330
15-06	25	4.28	20.8	4.24	330
16-06	26	4.29	25.5	4.22	332
17-06	27	4.30	25.6	4.23	331
18-06	28	4.30	25.5	4.23	331
19-06	29	4.28	25.6	4.21	333
20-06	30	4.28	24.9	4.22	332
21-06	31	4.28	25.7	4.21	333
22-06	32	4.31	25.6	4.24	330
23-06	33	4.28	25.5	4.21	333
24-06	34	4.28	25.9	4.21	333
25-06	35	4.31	29.7	4.21	333
26-06	36	4.31	29.5	4.21	333
27-06	37	4.31	30.1	4.21	333
28-06	38	4.31	29.5	4.21	333
29-06	39	4.32	29.5	4.22	332
30-06	40	4.34	33.8	4.21	333
01-07	41	4.34	34.7	4.21	333
02-07	42	4.33	33.0	4.21	333
03-07	43	4.34	29.5	4.24	330
04-07	44	4.32	30.1	4.22	332
05-07	45	4.33	32.8	4.21	333
06-07	46	4.34	32.8	4.22	332

07-07	47	4.33	32.8	4.21	333
08-07	48	4.33	32.8	4.21	333
09-07	49	4.37	38.4	4.21	333
10-07	50	4.34	34.7	4.21	333
11-07	51	4.38	38.4	4.22	332
12-07	52	4.39	38.7	4.23	331
13-07	53	4.40	38.4	4.24	330
14-07	54	4.38	34.7	4.24	330
15-07	55	4.37	34.5	4.24	330
16-07	56	4.40	38.4	4.24	330
17-07	57	4.37	34.0	4.24	330
18-07	58	4.40	38.4	4.24	330
19-07	59	4.38	37.3	4.23	331
20-07	60	4.41	42.8	4.22	332
21-07	61	4.43	46.4	4.21	333
22-07	62	4.43	45.2	4.22	332
23-07	63	4.42	42.0	4.23	331
24-07	64	4.42	45.6	4.21	333
25-07	65	4.43	45.8	4.22	332
26-07	66	4.46	46.4	4.24	330
27-07	67	4.46	46.4	4.24	330
28-07	68	-	-	-	-
29-07	69	-	-	-	-
30-07	70	-	-	-	-
31-07	71	4.45	46.4	4.23	331
01-08	72	4.45	46.4	4.23	331
02-08	73	4.45	45.4	4.24	330
03-08	74	4.45	45.4	4.24	330
04-08	75	4.45	45.2	4.24	330
05-08	76	4.45	45.4	4.24	330
06-08	77	4.43	42.0	4.24	330
07-08	78	4.46	46.6	4.24	330
08-08	79	-	50.0	-	-
09-08	80	-	45.4	-	-
10-08	81	-	50.0	-	-
11-08	82	-	50.0	-	-
12-08	83	-	45.9	-	-
13-08	84	-	34.4	-	-
14-08	85	-	29.5	-	-
15-08	86	-	24.9	-	-
16-08	87	-	17.7	-	-
17-08	88	-	4.1	-	-
18-08	89	-	1.6	-	-
19-08 | 24-09	90 | 126	-	1.0	-	-

Tab. 3. Results of the measurements using the passive system (unit #3)

Date	Time	Time of propagation	Sound velocity
	days	ms	m/s
21-05	0	1.928	322
28-05	7	1.924	322
4-06	14	1.920	322
12-06	22	1.928	321
18-06	28	1.900	326
25-06	35	1.888	328
2-07	42	1.900	326
9-07	49	1.896	327
16-07	56	1.900	326
25-07	65	1.888	328
31-07	71	1.892	327
6-08	77	1.884	329
13-08	84	-	-
20-08	91	-	-
27-08	98	-	-
3-09	105	-	-
18-09	120	-	-
24-09	126	-	-